JOURNAL OF AGRICULTURAL AND FOOD CHEMISTRY

Article

pubs.acs.org/JAFC

Structure and Physical Properties of Zein/Pluronic F127 Composite Films

Ji Li, Yunqi Li, Tung-Ching Lee, and Qingrong Huang*

Department of Food Science, Rutgers University, 65 Dudley Road, New Brunswick, New Jersey 08901-8520, United States

Supporting Information

ABSTRACT: Triblock copolymer Pluronic F127 has been used to form composites with zein, a corn protein and coproduct of the bioethanol industry, to alleviate its natural brittleness. At low F127 loadings (0−35%), the plasticizing effect was dominant, and the elongation at break of zein composite film containing 35% F127 was about 8-fold higher than that of the zein film with 10% F127. At high F127 loadings (50−100%), a large number of lamellae crystals were formed in the film matrix as verified by a combination of differential scanning calorimetry (DSC), atomic force microscopy (AFM), and small-angle X-ray scattering (SAXS). The F127 crystallization surpassed its plasticizing effect, resulting in an increased brittleness of zein film with the further increase of F127 loading. Compared with the flat-on lamellae of pure F127, F127 chains folded into branch-like lamellar structures in the zein composite film containing 50% F127 due to the confinement of amorphous zein. Besides, the crystals in zein films were composed of extended chain integral folding (IF = 0) and once-folded chain (IF = 1) polyethylene oxide (PEO) crystals, and the portion of once-folded chain (IF = 1) PEO crystals increased with F127 loading. Thus, through investigation of the competition of plasticizing effect and crystal formation under different F127 loadings, the optimized F127 loading in zein/F127 composite film with a good overall performance was determined to be at around 35%.

KEYWORDS: *zein, Pluronic F127, plasticizing effect, crystallization, composite films*

INTRODUCTION

Nowadays, the majority of packaging materials are petroleum-based polymers at the expense of sustainability and environmental protection.[1] To alleviate the environmental pressure caused by petroleum-derived materials, researchers are actively searching for substitutes for those environmentally unfriendly polymers from renewable resources such as polysaccharides, proteins, and microbial-fermented polymers.[2] The investigation of those biopolymers matches the trend of novel material development, which is marked with the keywords "functional", "environment-friendly", and "green chemistry".[3−5]

Among natural biopolymers, corn protein zein is a film-forming material that can potentially be utilized for packaging applications if its natural brittleness can be improved. In addition, zein also displays other advantageous physical properties including toughness, hydrophobicity, and microbial resistance.[6] Unlike globular protein, zein has different solution behaviors that have been investigated by several groups.[7−9] Early, Tatham et al. determined that the radius of gyration (R_g) of zein in 70% (v/v) aqueous methanol solution was 4.4 nm with a radius of gyration of the cross-section (R_c) of 0.25 nm.[9] Later, Matsushima et al. broke down the disulfide bond between Z19 and Z22 in an α-zein mixture by β-mercatopethanol. From their small-angle X-ray scattering (SAXS) results, they established a tetramer model for α-zein Z22, which consisted of 10 antiparallel helices with a reasonable axial ratio of 6:1.[8] This zein model was later supported by Momany et al.[10] Very recently, by analyzing the concentration-dependent R_g obtained from SAXS and apparent viscosity data from rheological measurements, Li et al. observed two distinct scaling regions of zein in acetic acid under the same critical concentration.[7] In addition, our recent study indicated that the different solvents (ethanol/water mixtures of different ratios versus acetic acid) could have significant impacts on the surface morphology of zein films.[11]

Although we are getting a clearer picture of zein's solution behavior, its natural brittleness still limits its further industrial applications as biodegradable packaging materials or edible films. The conventional approaches to improve the flexibility of zein include either chemical modification[12] or the formation of composite films through the addition of low molecular weight plasticizers.[13,14] Compared with the chemical modification approach, the formation of biopolymer composite films is an economical and convenient method for optimizing the overall performance of biopolymer product with the combined advantages of each component involved. Because most polymers cannot form completely compatible blends,[15] the challenge for preparing biopolymer composite films largely depends on the selection of polymer components. Previously, different small molecules (e.g., sugars,[16] polyethylene glycol 300,[14] and fatty acids[17]) and different synthetic polymers (e.g., polyvinylpyrrolidone,[18] nylon-6,[19] and polyvinyl alcohol[20]) have been used to improve the mechanical properties of zein. Ghanbarzadeh et al. compared the softening effect of different sugars such as fructose, galactose, and glucose on zein films. Their tensile test results showed fairly large Young's modulus and small elongation at break values, indicating a relatively small plasticizing effect of sugar.[16] Santosa and Padua utilized oleic acid and linoleic acid as plasticizers to soften zein film.[17]

Received: October 8, 2012
Revised: January 22, 2013
Accepted: January 23, 2013
Published: January 23, 2013

Those fatty acid-plasticized zein films also required an additional replasticization process, which was time-consuming. Selling et al. pioneered the formation of zein composites with synthetic polymers such as PVP[18] and nylon-6.[19] The very first trial was a zein/PVP composite film.[18] From their paper, the addition of a 55 kDa PVP into zein film enhanced the tensile strength of zein film by 24%.[18] However, the elongation at break of zein/PVP blend film displayed no significant improvement compared with that of pure zein film. In another report, Selling et al. blended zein with 2−8% nylon-6 and found that the tensile strength of zein film was improved by 33%, and the solvent resistance of zein films to 90% ethanol/water was also found to be better.[19] However, the elongation at break of zein/nylon-6 films was still of the same order as that of the pure zein film, indicating no significant improvement in flexibility. Several mechanical tests were accomplished with the aid of combined plasticizers such as tri(ethylene glycol)[19] and air moisture,[18] because tri(ethylene glycol) and water could effectively interact with zein[21] and further alleviate zein's natural brittleness or low flexibility. In addition, few formulations have been investigated clearly from the viewpoints of both macroproperty level and microstructure level.

In this paper, we aim to improve the flexibility of zein film and simultaneously understand the structure−property relationship behind it. We prepare zein/Pluronic F127 composite films to optimize the mechanical properties of the resulting zein films and then systematically investigate the microstructures of zein/F127 composite films under different F127 loadings. As a blending component, Pluronic F127 is an amphiphilic surfactant with a chemical composition of poly(ethylene oxide)$_{98}$−poly(propylene oxide)$_{67}$−poly(ethylene oxide)$_{98}$ (PEO_{98}−PPO_{67}−PEO_{98}). It has been widely studied for its solution behavior,[22,23] unique polymorphism,[24] sol−gel transition,[25] and applications in drug delivery.[26] Pluronic F127 not only shows biocompatibility itself[27] but also helps to improve functionalities of other biomaterials such as myoglobin.[28] In liquid, Pluronic F127 exhibits an excellent capability as a stabilizing agent for drug delivery;[29] whereas in solid, it serves as a structure-directing agent for silica film with controlled three-dimensional porous structure.[30,31] Because of its biocompatibility, predictable structures in both solid and liquid, and low glass transition temperature, Pluronic F127 was selected as a plasticizer and film-forming enhancer to form composite films with zein. The interaction, miscibility, structure, surface hydrophobicity, and surface morphology of the zein/F127 composites were investigated by a combination of Fourier transform infrared spectroscopy (FTIR), differential scanning calorimetry (DSC), small-angle X-ray scattering (SAXS), and atomic force microscopy (AFM). The thermal and mechanical properties as well as the microstructures of zein/F127 composite films have been systematically studied. The structure−property relationship of zein/F127 composite films at different F127 loadings was established, which can benefit the future design of other protein-based biomaterials.

MATERIALS AND METHODS

Materials. Zein powder containing ∼95% α-zein was purchased from Wako Corp. Pluronic F127 NF Prill Poloxamer 407 was a gift obtained from BASF Corp. Acetic acid (glacial, ACS grade) was purchased from Fisher Chemical. All of the reagents were used as received.

Preparation of Zein/F127 Composite Films. The stock solutions of zein and F127 were prepared in pure acetic acid at the concentration of 100 mg/mL. After full dissolution of zein and F127 in acetic acid, the stock solutions of zein and F127 were filtered through 0.45 μm polytetrafluoroethylene (PTFE) filters to remove impurities. F127 solution was added into zein solution dropwise to achieve F127 loadings ranging from 0 to 100%. Films with 0 and 100% F127 loading refer to pure zein and pure F127 samples, respectively. Then zein/F127 liquid mixtures were poured into highly flat Teflon Petri dishes. After staying at room temperature for 2 h to avoid film surface defects arising from fast solvent evaporation, those Petri dishes were placed in a 50 °C oven overnight and then dried in a 40 °C vacuum oven for another 24 h. The transparency of the final zein/F127 composite films was dependent upon F127 loading. When F127 loading reached 75%, the film became opaque due to the formation of F127 crystals.

Surface Morphology Analyses. Surface morphological images of zein/F127 composite films were collected using a commercial Nanoscope IIIa Multi-Mode AFM (Veeco Instruments, Camarillo, CA, USA) equipped with a J scanner, which was operated in tapping mode using a silicon cantilever. Both height and phase images were collected simultaneously using a set point ratio of ∼0.9 for measurements at room temperature. At least 10 local spots on each film sample were imaged with the scan size of 10 μm × 10 μm. Thus, the AFM results can represent the overall surface morphology. The root-mean-square (RMS) surface roughness of each zein/F127 composite film was calculated using Nanoscope software 5.30.

Thermal Analyses. The thermal properties of the dried zein/F127 composite films were determined by a DSC 823E thermal analyzer (model 823, Mettler Toledo Instruments, Columbus, OH, USA). The films were cut into small pieces prior to experiments. DSC thermograms were collected by a two-cycle mode with 5−8 mg samples at the scan rate of 10 °C/min and a compressed nitrogen purge of 60 mL/min. For the first cycle, the samples were heated from 25 to 200 °C to remove the thermal history and then cooled from 200 to −100 °C. The second cycle scanning started from −100 to 200 °C at the same scanning rate. For each zein/F127 composite film, the melting temperature (T_m) of F127 was obtained as the peak temperature, whereas the glass transition temperature (T_g) of zein was the midpoint between the onset temperatures during second-cycle scanning. Also, the T_m of pure F127 and the T_g of pure zein were used as references after the DSC analyses of pure F127 film and pure zein film. Besides, the enthalpy of crystalline melting (ΔH) was calculated using the area under curve of the melting peak and then normalized by the weight fraction of PEO blocks in the composite films.

Mechanical Properties. Tensile test was performed for zein/F127 composite films. The elastic modulus, tensile strength, and elongation at break of the films were measured by *TA.XT2i* Texture Analyzer (Texture Technologies Corp., Scarsdale, NY, USA) according to EN ISO 527-3: 1995 E at a speed of 5.0 mm/min. The films were carefully cut into rectangular shape with a dimension of 1.0 mm × 60.0 mm. The film thicknesses were between 0.3 and 0.4 mm. The initial gap was set at 25.0 mm. The film samples were subject to tensile test right after vacuum annealing. All of the measurements were replicated at least three times for each sample.

ATR-FTIR Spectroscopy. The attenuated total reflectance Fourier transform infrared (ATR-FTIR) spectra of film surfaces were collected under ambient condition by utilizing a Thermal Nicolet Nexus 670 FT-IR spectrometer (Thermo Fisher Scientific Inc., Waltham, MA, USA) equipped with a Smart MIRacle horizontal attenuated total reflectance Ge crystal accessory. Each spectrum was averaged over 512 scans with 4 cm^{-1} resolution.

Small-Angle and Wide-Angle X-ray Scattering. Small-angle and wide-angle X-ray scattering data were collected at the 18-ID beamline of BIO-CAT, at the Advanced Photon Sources, Argonne National Laboratory, Argonne, IL, USA. The film samples with surfaces perpendicular to the X-ray beam were directly positioned in the optical path of the X-ray beam. For SAXS, the sample−detector distance was fixed at 0.826 m, which was utilized to cover a scattering vector Q range of 0.01−0.35 $Å^{-1}$. For WAXS, the sample-to-detector distance is set at 180 mm, which corresponds to a Q range of 0.08−2.5 $Å^{-1}$. A Mar165 CCD was installed lateral to the X-ray beam. The X-ray wavelength was 1.033 Å ,and the energy of X-ray was 12 keV. A single

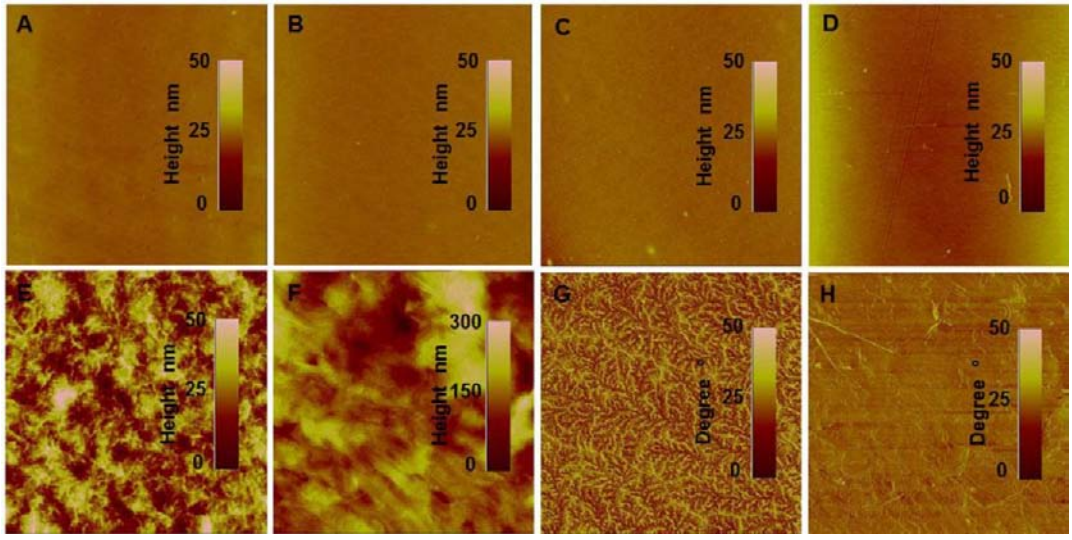

Figure 1. Tapping mode atomic force microscopy (TPAFM) images of zein/F127 composite films with different F127 loadings. Height images: (A) 0% F127; (B) 10% F127; (C) 20% F127; (D) 35% F127; (E) 50% F127; (F) 100% F127. Phase images: (G) 50% F127; (H) 100% F127. The scan size is fixed at 10 μm × 10 μm.

exposure of 1 s was used to obtain the scattering data. The background for films was air at room temperature. Three structural parameters of Pluronic F127 including PEO volume fraction in block copolymer φ_{PEO}, chain length in liquid γ_v, and order-to-disorder transition temperature T_{ODT} were calculated to be 66%, 295, and 169 °C, respectively.[32] Therefore, Pluronic F127 should form ordered structure at room temperature.

The crystalline phases in the composite films were determined from the relative positions of the SAXS peaks. For lamellar structures, the peak positions should obey the relationship of 1:2:3:4, etc. The structure parameter d (average long periodicity) was obtained from the position (q^*) of the first (and the most intense) diffraction peak. The equation of average long periodicity d is shown as follows:

$$d = \frac{2\pi}{q^*} \tag{1}$$

In the lamellar phase, the average long periodicity d is quantified from the inverse film area (A) per volume (V) ratio. This A/V ratio of the local copolymer film is given by eq 2.[33,34] Assuming a clear interface between hydrophilic PEO and hydrophobic PPO, we calculate the interfacial area α_p, the effective area per PEO block at the interface between polar and apolar domains, by eq 3

$$A/V = 2\varphi_p\alpha_p/V_p \tag{2}$$

$$\alpha_p = \frac{V_p}{d\varphi_p} \tag{3}$$

where φ_p is the polymer volume fraction, α_p is the effective interfacial area per PEO block, and V_p (≈19933.6 Å^3) is the estimated volume of one F127 polymer molecule based on the calculation method of one Pluronic P105 volume.[33]

Statistical Analysis. SigmaPlot 11.0 software with SigmaStat integration (Systat Software) was used to perform all of the statistical analysis. One-way analysis of variance (ANOVA) tests were followed by the Holm−Sidak method, with the overall significance level set at 0.05. Non-normal raw data were first transformed to meet the requirement of ANOVA.

RESULTS AND DISCUSSION

Surface Morphology. The surface morphologies of zein/F127 composite films were collected using tapping mode AFM, and typical morphologies at different F127 loadings are presented in Figure 1. At low F127 loadings (Figure 1A−D), the film surfaces were flat and featureless. These flat surfaces are consistent with our previous observation of flat zein thin films being achieved by spin-cast on silicon wafer.[11] At high F127 loadings (50−100%), large amounts of lamellae crystals were observed (Figure 1E−H). Interestingly, edge-on or branch-like lamellae crystals were found in the zein/F127 composite film with 50% F127 loading (Figure 1E,G). For comparison, a 100% F127 crystalline pellet is also shown in Figure 1. It is clear that flat-on lamellae crystals are spread all over the pellet surface in panels F and H of Figure 1. The difference of geometries between flat-on and edge-on lamellae lies in the crystal orientation. The crystal growth that follows a c-axis orientation generates flat-on lamellae, whereas crystals oriented in $a-b$ plane have edge-on lamellae. The basic structures of flat-on and edge-on lamellaes are the same, but just one is tilted 90° from another. Growth of lamellae crystals in different environments results in the observation of different surface morphologies. Without any external restriction, semicrystalline F127 can naturally stretch into flat-on lamellae, which is in agreement with the mean-field prediction of F127 melt at room temperature (Figure 1F,H).[35−37] As a blending partner, the amorphous zein not only occupies a certain amount of space in the bulk film but also interacts with F127 through a couple of possible interactions (i.e., hydrogen bonding and hydrophobic interaction). Under such circumstances, the growth of F127 lamellae crystals is restricted by amorphous zein's geometry and its interaction with zein in the bulk film. Therefore, the confinement of amorphous zein shapes polyether chains to fold into branch-like geometry (Figure 1E,G). The details of F127 crystals confined by zein will be discussed in more detail later.

The RMS surface roughness of the zein/F127 composite films is shown in Figure 2. With the increase of F127 loading from 0 to 75%, the averaged RMS roughness of zein films increased from 2 to 12 nm, indicating the surface roughening induced by F127 crystals. The roughness of the pure F127 crystal pellet with a high value of 77.7 nm is shown as a reference value in Figure 2. Our results suggested that the film surfaces at high F127 loadings were very likely covered by crystalline PEO blocks of F127. Such spatial distribution of

dx.doi.org/10.1021/jf3043055 | J. Agric. Food Chem. 2013, 61, 1309−1318

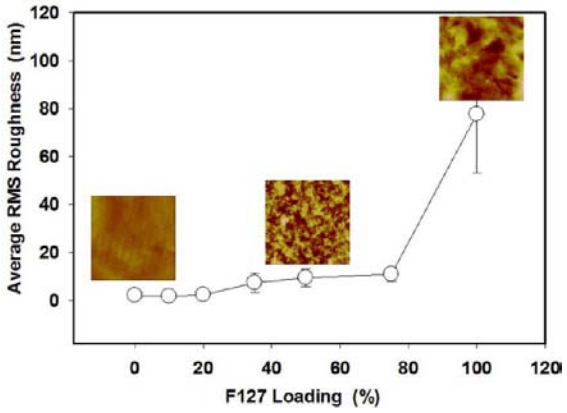

Figure 2. Plot of averaged root-mean-square (RMS) roughness of zein/F127 composite film surfaces versus F127 loadings. (Insets) Tapping mode atomic force micrscopy height images of zein/F127 composite films with F127 loadings of 0, 50, and 100%, respectively.

F127 in the bulk film, in which each component tends to stay in the bottom or upper space, may be driven by gravity, surface tension, and other molecular interactions (i.e., hydrogen bonding and hydrophobic interaction). Because the bulk density of zein is estimated to be >1.36 g/mL[38] and the density of F127 is 1.05 g/mL, gravity exerts more impact on zein than F127. Hence, it is not unexpected to observe the F127-covered film surface due to the gravity role during solvent evaporation. Besides, due to hydrophilicity and self-crystallization, the PEO block has lower miscibility than PPO to zein; thus, it tends to segregate from the hydrophobic regions of zein and PPO and then enriches the film surface. The segregation of PEO blocks onto the air/solid interface is also due to the difference of surface tension between zein, PPO, and PEO ($\gamma_{PEO} > \gamma_{PPO}$ and γ_{zein}). A similar phenomenon of block segregation was also observed in the poly(styrene)-*b*-poly(methyl methacrylate) (PS-*b*-PMMA) film as well.[39]

Thermal Analyses. Most zein composite films with low F127 loadings are transparent (see Figure S1 in the Supporting Information), suggesting that zein and F127 have a certain degree of miscibility. Such miscibility is probably attributed to the hydrogen bonding and hydrophobic interaction between PPO block in F127 and hydrophobic residues in zein.[7] The partial miscibility of PPO block and zein may confine the crystallization of PEO block in F127, causing a shift in melting temperature (T_m) and glass transition temperature (T_g). We then utilized DSC to detect such changes from the T_m of pure F127 (~56 °C) and the T_g of pure zein (~97 °C) (Table 1).

Table 1. Thermal Properties of Zein/F127 Composite Films

F127 loading (%)	T_g (°C)	T_m (°C)
0	97.1 ± 1.6	NA[a]
10	95.5 ± 0.7	NA[a]
20	90.9 ± 0.8[b]	47.6 ± 3.0
35	88.4 ± 0.9[b]	53.4 ± 0.1
50	84.9 ± 3.3[b]	51.5 ± 5.9
75	NA[c]	55.2 ± 1.8
100	NA[c]	56 ± 0.0

[a] T_m is not observable on the endothermal curve due to the amorphous structure. [b] Significant difference from the pure zein film. [c] T_g is not observable on the endothermal curve due to the large melting peak of F127 and low amount of glassy zein.

Figure 3A shows the DSC thermograms of zein/F127 composite films with different F127 loadings. For comparison, the DSC thermogram of pure F127 is listed in Figure S2 of the Supporting Information. The T_m of the composite film was depressed when F127 loading decreased. Besides, the change of T_g in the composite film was also affected by the F127 loading. Because the T_g change was less observable than T_m in the same plot, we replotted the typical glass transition curves of zein/F127 composite films for clearer observation (Figure 3B). With an increase of F127 loading, the decrease of T_g also suggested the partial miscibility between zein and F127 (Figure 3B). In addition, the melting enthalpy (ΔH) is relevant to crystallinity. Figure 3C shows the impact of F127 loading on the melting enthalpy. The nonlinear decrease of ΔH with F127 loading indicated the existence of different crystal growth stages at different F127 loadings.

Table 1 lists the detailed thermal properties of zein/F127 composite films with different F127 loadings. The T_g of pure zein film was 97 °C, which was in agreement with the previous thermal results.[12] With an increase of F127 loading from 0 to 35%, the T_g of zein dropped from 97.0 to 88.4 °C. In addition, the T_g of zein/F127 composite film with 35% F127 was significantly lower than that of pure zein film. The T_m values of the composite films decreased from 55.2 to 47.6 °C when the F127 loading decreased from 75% to 20%. Such changes of T_g and T_m resulted from the miscibility of PPO block and zein that suppressed the space for the crystallization of PEO block, which further caused the decrease of crystal size and introduced imperfections in the crystal structure.

Mechanical Properties. A tensile test was conducted to determine the mechanical properties of zein/F127 composite films. Figure 4 exhibits the stress–strain curves of zein/F127 composite films with different F127 loadings. The elongation at break of the zein/F127 composite films was enhanced >8-fold (from <10% to >82%) when F127 increased from 10 to 35%. However, further increase of F127 loading to 50% brought a deleterious impact on the elongation of the film. The tensile strength, elongation at break, and elastic modulus of these films are presented in Table 2. The variation of these three parameters is likely due to the difference in film thickness. It can be seen that the loading of F127 has a significant impact on the mechanical properties of zein/F127 composite films. Among those films, the film with 35% F127 exhibited the lowest values of tensile strength (9.2 MPa) and elastic modulus (163 MPa) and simultaneously showed the highest elongation at break (92.0%). The values of tensile strength, elastic modulus, and elongation at break of zein/F127 composite film with 35% F127 were significantly different from those of zein/F127 composite film with 10% F127. The decreases of tensile strength and elastic modulus verified the plasticizing effect of F127 on the composite film. Hence, 35% F127 loading reaches the maximum plasticizing effect of F127 due to its interaction with zein in the amorphous region. At high F127 loading, the crystalline nature of F127 dominated the plasticizing effect of F127, causing the increased brittleness of the composite films.

Conventionally, different plasticizers such as glycerol, sugars, and fatty acids have been employed to improve the mechanical properties of zein films. Comparison of our films with those reported plasticized films[14,17,40] reveals remarkable advantages. Those fatty acid- or sugar-plasticized zein films are either less effective or tedious in sample preparation. In contrast, Pluronic F127 surfactant exhibited a better plasticizing effect with

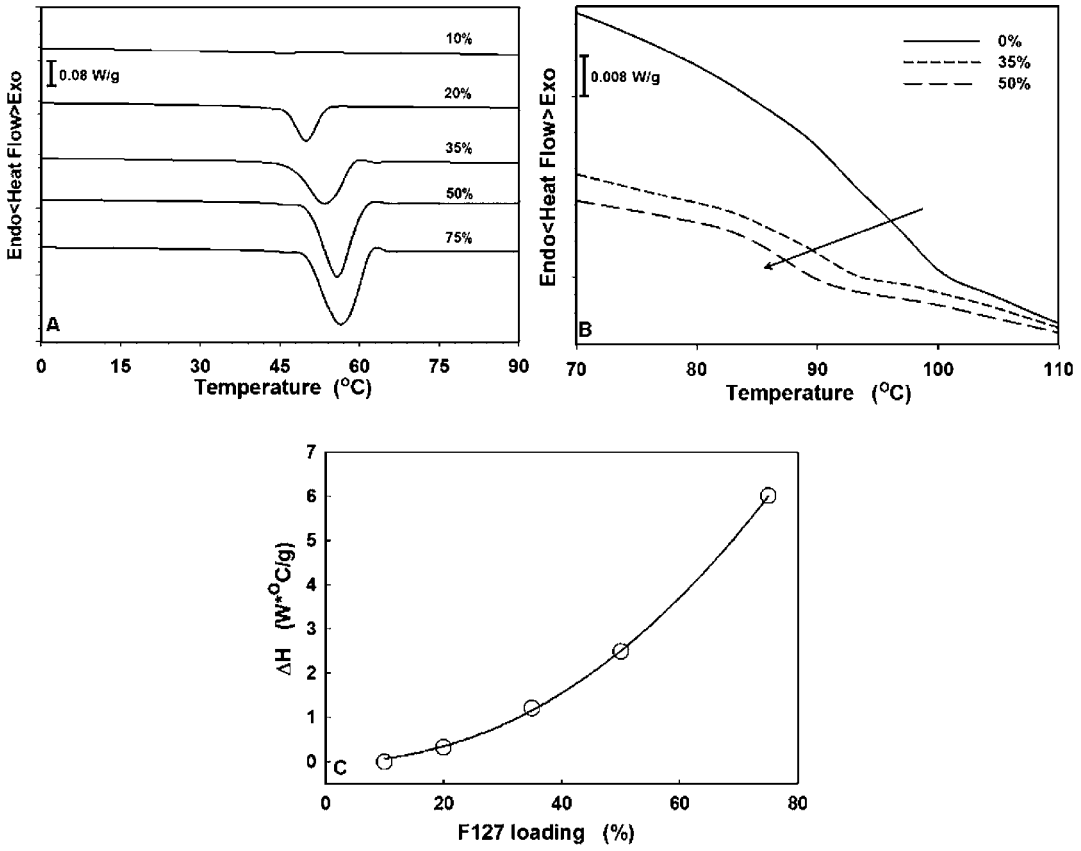

Figure 3. (A) Melting temperature (T_m) alternation of zein/F127 composite films with different F127 loadings (10−75%); (B) glass transition temperature (T_g) change of zein/F127 composite films with different F127 loadings (0, 35, and 50%); (C) plot of the crystalline melting enthalpy (ΔH) versus F127 loading. The solid line in (C) is used to guide the eyes.

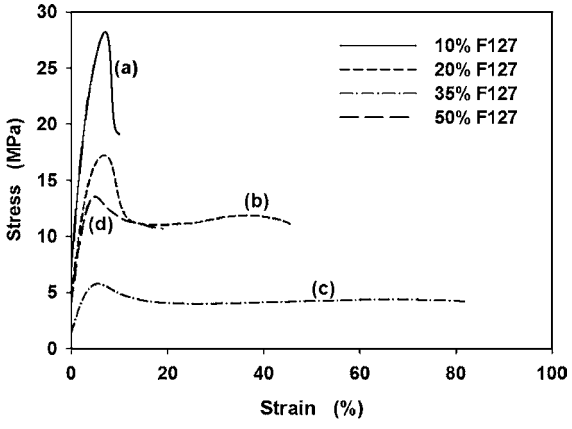

Figure 4. Tensile stress−strain curves of zein/F127 composite films with F127 loadings of (a) 10%, (b) 20%, (c) 35%, and (d) 50%.

Table 2. Mechanical Properties of Zein/F127 Composite Films

F127 loading (%)	tensile strength (MPa)	elongation at break (%)	elastic modulus (MPa)
10	29.1 ± 2.0	16.0 ± 2.7	468.1 ± 22.4
20	20.1 ± 1.6[a]	45.0 ± 14.9[a]	291.8 ± 33.3[a]
35	9.2 ± 1.4[a]	92.0 ± 9.6[a]	163.0 ± 26.7[a]
50	17.0 ± 1.6[a]	16.0 ± 3.3	258.0 ± 16.8[a]

[a]Significant difference from the zein/F127 composite film with 10% F127 loading.

convenient preparation. The mechanical test here suggests that at proper loading level, F127 can effectively reduce the brittleness of zein film due to the partial miscibility of zein and F127 at the amorphous region, which also ensures the integrity of zein's structure as well.

Molecular Interaction in Zein/F127 Composite Films. Figure 5A shows the ATR-FTIR spectra (4000−600 cm^{-1}) from the surface of zein/F127 composite films with different F127 loadings. The characteristic peaks of F127 located at 1342 cm^{-1} (−CH_2 wag), 1279 cm^{-1} (−CH_2 twist), 1104 cm^{-1} (C−O−C stretching), and 962 cm^{-1} (−CH_2 rock) were in agreement with previous results.[41] The two peaks located at 1649 and 1536 cm^{-1} corresponded to the amide I band and amide II band of zein.[42] The absorption peaks at 3000−2880 cm^{-1} (C−H stretching) were sensitive to the F127 chain. With the increase of F127 loading, the 2959 cm^{-1} peak (C−H asymmetric stretching vibration of −CH_3) disappeared and the 2883 cm^{-1} peak (symmetric stretching vibration of −CH_2) grew gradually, which were probably attributed to the segregation of PEO blocks (−O−CH_2CH_2) on the composite film surface, because ATR-FITR majorly scanned the film surface. When F127 increased from 0% to 35%, a strong increase of the broad peak at 3292 cm^{-1} was found due to the increased amount of hydroxyl groups (−OH) in the zein/F127 composite films. Additionally, this broad peak shifted to a lower wavenumber, indicating that the addition of F127 led to different patterns of hydrogen bonding.

To further investigate hydrogen bonding in the zein/F127 composite films, the Fourier deconvolution plots of −OH and −NH_2 bands are shown in Figure 5B for pure zein film and in

dx.doi.org/10.1021/jf3043055 | J. Agric. Food Chem. 2013, 61, 1309−1318

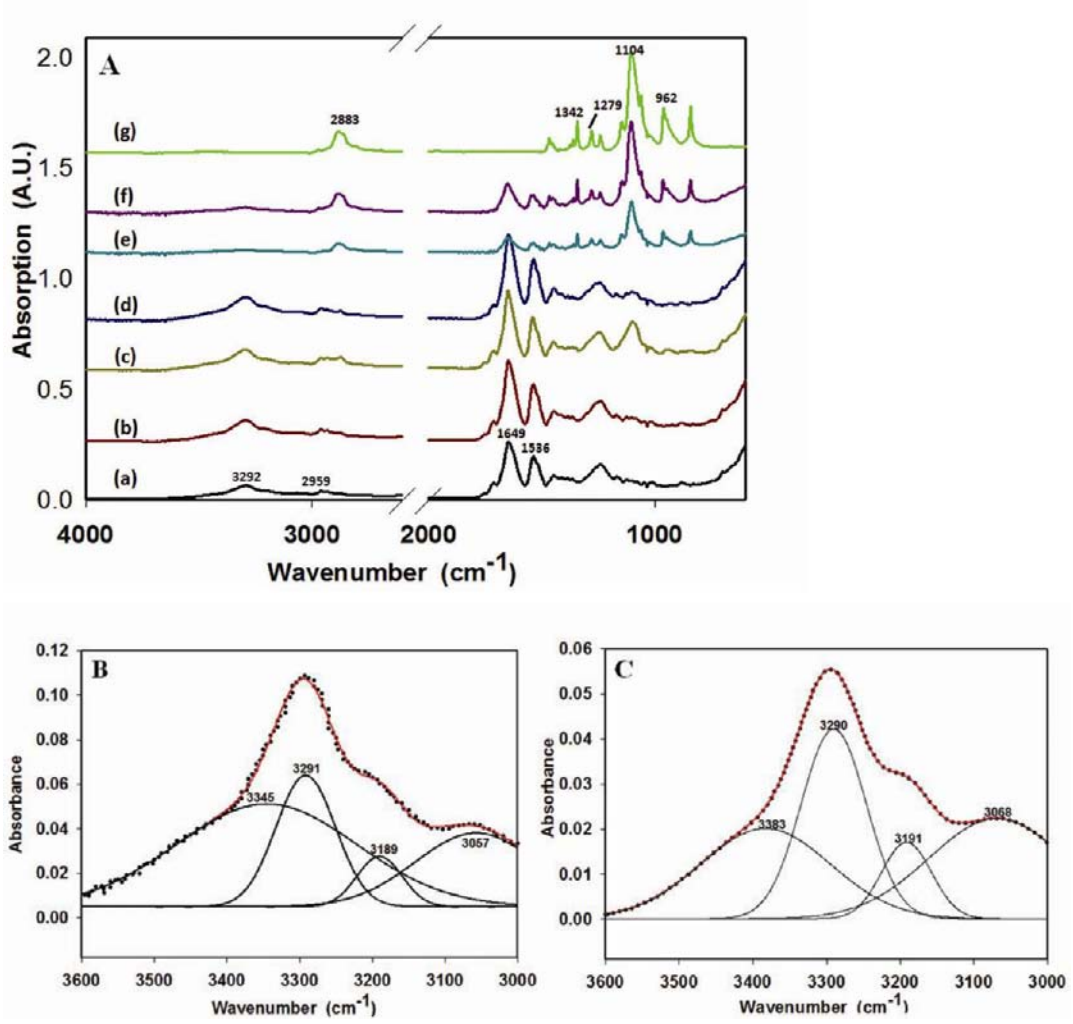

Figure 5. (A) Fourier transform infrared spectra of zein/F127 composite films with F127 loadings of (a) 0%, (b) 10%, (c) 20%, (d) 35%, (e) 50%, (f) 75%, and (g) 100% within the wavenumber range of 4000−600 cm^{-1}. Best fit curves for the self-deconvoluted FTIR spectra using nonlinear regression analyses: (B) overlapped −OH, $-NH_2$, and CH stretching bands (3600−3000 cm^{-1}) in pure zein film (0% F127 loading) and (C) zein/F127 blend film (35% F127 loading). The hydrogen bonding band was fitted with Gaussian functions using peak positions obtained from second-derivative analysis.

Figure 5C for composite film with 35% F127 loading. Four peaks at 3345, 3291, 3189, and 3057 cm^{-1} were assigned to the stretching of −OH in intramolecular and intermolecular hydrogen bonding, $-NH_2$ in hydrogen binding, and the stretching of −C−H. The area ratio of those four bands for pure zein film (0% F127 loading) was 43.8:23.2:12.0:21.0, indicating a large contribution from intramolecular hydrogen bonding. From 35% F127 composite film, these corresponding peaks shifted to 3383, 3290, 3191, and 3068 cm^{-1}, respectively, and the ratio changed to 30.4:32.2:10.0:27.4. This suggested that intermolecular hydrogen bonding between F127 and zein dominated the intramolecular hydrogen bonding of zein. Table 3 summarizes the contribution from these four typical interactions in the zein/F127 composite films. The F127 loading had little impact on the contribution of hydrogen-bonded $-NH_2$ and −CH stretching components. Clearly, by increasing F127 loading from 0 to 10, 20, and 35%, the component of intramolecular hydrogen bond −OH decreased, whereas intermolecular hydrogen bond −OH contributed more to the hydrogen-bonding profile. Also, compared with pure zein film, zein/F127 composite films with low F127 loadings (10−35%) display significant differences of intramolecular hydrogen bond and intermolecular hydrogen bond. This phenomenon indicates that intermolecular hydrogen bond greatly contributes to the miscibility of zein and F127 at low F127 loading composite films.

Table 3. Hydrogen Bonding Profiles of Zein/F127 Composite Films with Low F127 Loadings

F127 loading (%)	$N_{intra\text{-}OH}$ (%)	$N_{inter\text{-}OH}$ (%)	N_{NH_2} (%)	N_{CH} (%)
0	43.8 ± 0.1	23.3 ± 0.1	12.0 ± 0.1	21.0 ± 0.1
10	32.0 ± 0.1[a]	32.2 ± 0.1[a]	9.8 ± 0.1	26.0 ± 0.1
20	36.3 ± 0.1[a]	30.4 ± 0.1[a]	9.6 ± 0.1	23.6 ± 0.1
35	30.4 ± 0.1[a]	32.2 ± 0.1[a]	10.0 ± 0.1	27.4 ± 0.1

[a]Significant difference from pure zein film.

Microstructure in Zein/F127 Composite Films. Because Pluronic F127 can self-assemble to form ordered structure, we applied small- and wide-angle X-ray scattering to study the microstructure of the composite films. Figure 6A presents the SAXS profile of pure F127, which has two clearly observable Bragg's peaks with the peak position (q^*) ratio of 1:2 in q-space. The first two peaks correspond to the first- and second-

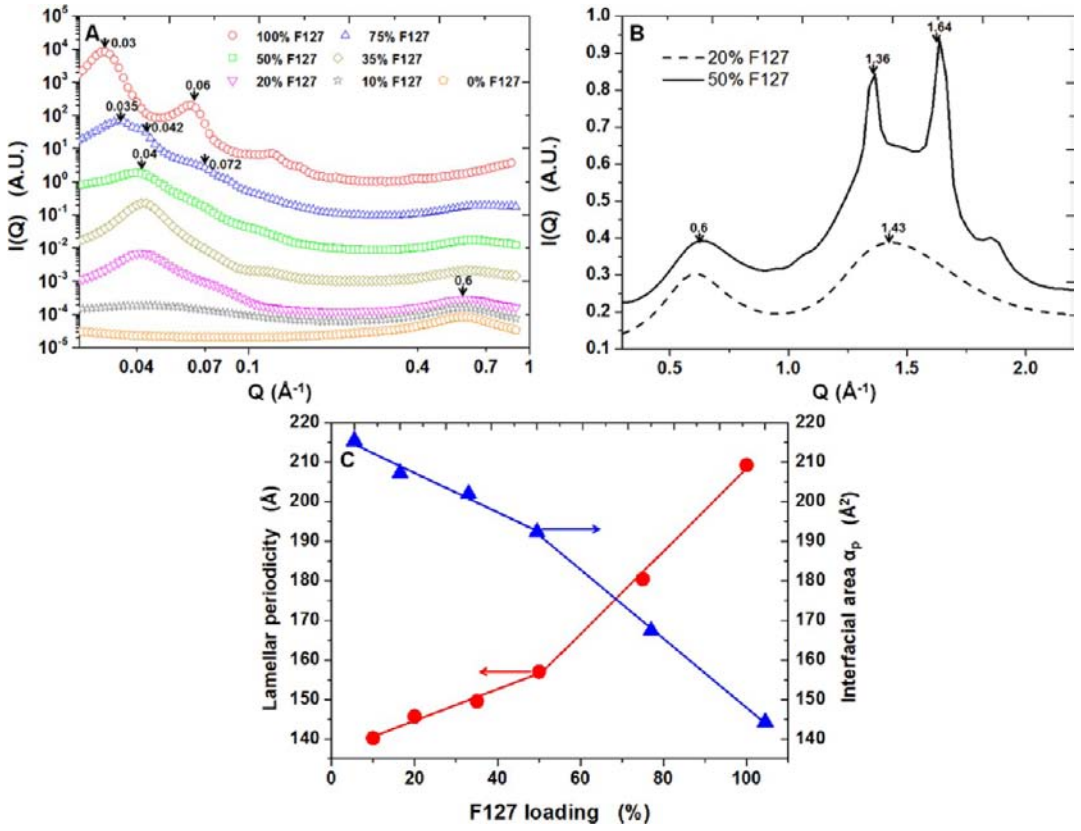

Figure 6. (A) Small-angle X-ray scattering (SAXS) profiles of zein/F127 composite films with different F127 loadings (10−100%); (B) wide-angle X-ray scattering (WAXS) profiles of zein/F127 composite films with F127 loadings of 20% (dash line) and 50% (solid line); (C) plots of averaged long periodicity d (solid circles) and polar−apolar interfacial area α_p (solid triangles) versus F127 loading for the zein/F127 composite films.

order lamellar structures in the film. Such ordered structure is consistent with the AFM images shown in panels F and H of Figure 1.

In terms of the microstructure of composite films, low F127 loadings (0−35%) are not enough to form highly ordered crystals in the zein-confined amorphous region, which is also reflected by tapping mode AFM images (Figure 1A−D). It is worth mentioning that a peak located at q = 0.6 Å^{-1} is observed for zein films with 0−20% F127 loadings, which corresponds to the intermolecular distance within the zein film (∼10.5 Å). High F127 loadings (50−75%) can result in the formation of highly ordered crystalline phase in the composite films. In Figure 6A, a composite film with 75% F127 loading displays two lamellar peaks similar to those of the pure F127 pellet. Different from the pure F127 pellet, the two peaks shifted to larger q region, indicating the formation of smaller crystals. Simultaneously, there is another shoulder peak located at q = 0.42 Å^{-1}, which may be due to other subtle metastable lamellar structure. For the film with 50% F127 loading, the first-order peak continued to shift to a larger q region and the second-order peak became less obvious, suggesting that the periodicity of lamellar order structure became less clear. The films with low F127 loadings (10−35%) display an even weaker first-order peak, which continued to shift to a larger q region.

Further application of WAXS to probe the structural change at the crystallite level is shown in Figure 6B. The peak at q = 0.6 Å^{-1} from the composite films of 20 and 50% F127 loadings overlaps with the peak observed in the SAXS profiles of zein films with 0−20% F127 loadings (Figure 6A), suggesting the intermolecular size of zein. From the composite film containing 50% F127, two sharp peaks at 1.36 and 1.64 Å^{-1} clearly indicate the formation of PEO crystals, whereas for the composite film containing 20% F127, only an amorphous halo was observed, suggesting a less ordered structure. A small amount of PEO crystallites can serve as nuclei for further crystallization. Similar WAXS profiles in consideration of the crystallization of PEO confined in the self-assembled nanoconfined lamellaes of PEO-*b*-PS copolymers have also been reported.[43]

On the basis of eqs 1 and 2, two lamellae parameters including long average periodicity d (d-spacing) and polar−apolar interfacial area α_p have been extracted from SAXS profiles (Figure 6A). Figure 6C exhibits the average long periodicity and interfacial area of zein/F127 composite films with different F127 loadings. Two linear increased trends were observed in the plot of d versus F127 loading and α_p versus F127 loading. As F127 increased from 10 to 50%, d increased from 140.1 to 157 Å, whereas α_p decreased from 2145.5 to 192.4 Å^2. At higher F127 loading (50−100%), the increase of d and decrease of α_p followed a sharper trend, suggesting two possible crystal growth stages (crystallite formation and crystal growth). The increase of periodic spacing d suggested that more F127 is involved in the lamellae construction with the increase of F127 loading. More F127 chains folded into lamellar structures and fewer F127 chains stayed at the interface between polar and apolar domains. Thus, the interfacial area between the amorphous region and the crystalline region decreased.

Understanding the Structure−Property Relationship. To understand the role of F127 on the structure and properties of zein/F127 composite films, we have studied the mechanical

dx.doi.org/10.1021/jf3043055 | J. Agric. Food Chem. 2013, 61, 1309−1318

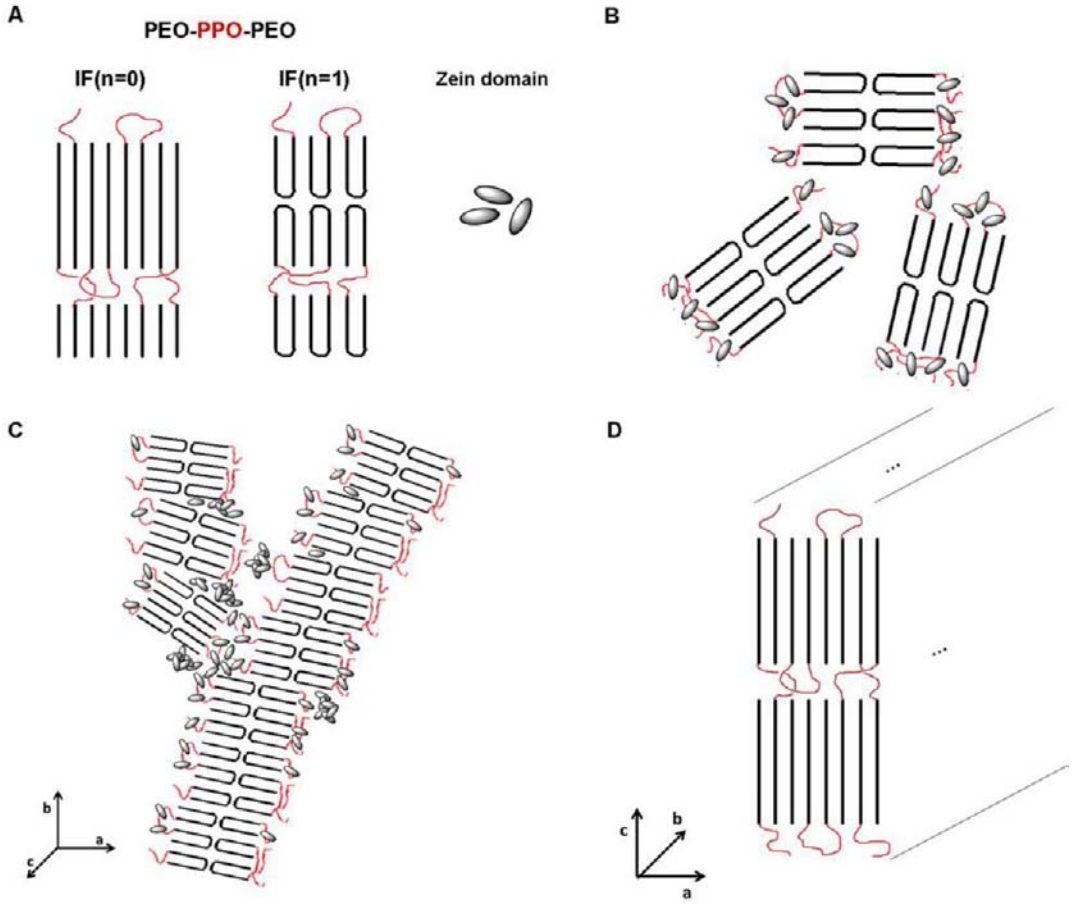

Figure 7. Mechanism of F127 crystallization in the zein/F127 composite films with different F127 loadings: (A) IF(n = 0) and IF(n = 1) crystal structures of PEO−PPO−PEO proposed by Zhang et al.[48] and zein domain in films; (B) crystallite formed at 20% F127; (C) branch-like (edge-on) lamellae formed at 50% F127 with eye perspective perpendicular (c axis) to the a−b plane; (D) flat-on lamellae formed at 100% F127 with eye perspective perpendicular to the a−c plane. The a−b plane is the film surface, whereas the c coordinate is perpendicular to the film surface.

properties and microstructure of the zein/F127 composite films at different F127 loadings. Both of them are tightly related to the crystallization of PEO under the confinement by PPO/zein aggregate domains. Besides, pure PEO (M_w = 4250 Da, a molecular weight almost equal to that of PEO portion in Pluronic F127) has been reported to have two types of crystals with different chain conformations.[44−47] Thus, we discuss the microstructure of the zein/F127 blend film and its impact on the film properties from two aspects: (1) confinement of PEO crystals and (2) integral-folding (IF) PEO chain conformation. Prior to further discussion, two types of crystals with different chain conformations are shown in Figure 7A. They are extended-chain IF(n = 0) crystal and once-folded chain IF(n = 1) crystal. The number n represents the PEO chain folding times. For the low molecular weight PEO fraction (M_w = 4250 Da), the number n is either 1 or 0.[48] Also, on the basis of the previously mentioned characterization results, we propose a possible crystallization mechanism of F127 at different loadings (Figure 7B−D).

At low F127 loadings (10−35%), the PEO blocks form very limited quantities of small crystallites, which are not enough for large crystal formation (Figure 7B). This can be verified by TP-AFM height images (Figure 1A−D) and low melting temperatures (Figure 3A). Meanwhile, the amorphous PPO blocks strongly interact with the zein domain through hydrogen bonding, which is supported by FTIR analysis (Figure 5B,C), and hydrophobic interaction. Because the matrix is a zein domain-dominant space, randomly distributed PEO crystallites cannot compete with the plasticizing effect provided by PPO−zein interaction. Hence, from macro length scale, we clearly observed the improved flexibility of zein film. Under such confinement of zein domain, PEO fractions of the triblock copolymers occupied space-saving conformation and eventually formed double-layer once-folded chain IF(n = 1) crystals. This argument can be supported by the long average periodicity d (d-spacing) (Figure 6C) calculated from the SAXS profiles (Figure 6A). At low F127 loading such as 20%, the d-spacing is 145 Å, which is almost identical to the fold length of IF(n = 1) crystals (slightly higher than 137 Å),[47] illustrating that the majority of PEO crystallites are chain-folded IF(n = 1) crystals. Because the melting temperature of IF(n = 1) crystals is reported to be lower than that of extended-chain IF(n = 0) crystals,[44,45,47] the low melting temperature (47.6 °C) observed from the DSC thermogram (Figure 3A and Table 2) also gives support to the dominance of IF(n = 1) crystals at low F127 loadings.

At a relatively high F127 loading such as 50%, the amount of PEO crystallites is enough to form higher order or larger crystals (Figure 7C). However, different from pure F127's flat-on lamellae, which grow in c orientation without confinement (Figure 7D), F127 chains are confined to grow in the a−b plane into branch-like large crystals. The interspace among

dx.doi.org/10.1021/jf3043055 | J. Agric. Food Chem. 2013, 61, 1309−1318

branches is fulfilled with zein domains. Those zein domains still interact with amorphous PPO segments along the branch contour. At this time, the brittleness caused by large amounts of branch-like crystals surpasses the plasticizing effect of F127, resulting in the shrunken elongation of film at macroscale. Meanwhile, with an increased amount of F127 in the film matrix, the larger space occupied by F127 results in an increasing portion of extended-chain IF(n = 0) crystals. The d-spacing of zein film at 50% F127 is 157 Å (Figure 6C), which is between the fold length of IF(n = 1) crystals (137 Å) and that of IF(n = 0) crystals (274 Å). However, that value of d-spacing is still close to the fold length of the IF(n = 1) crystal, suggesting the majority of once-folded chain IF(n = 1) crystals.

As a reference, a 100% F127 pellet is also studied along with other zein blend films. Its brittleness comes from the formation of large crystals, also called "flat-on" lamellae, which grows in c orientation without confinement (Figure 7D). Its typical surface morphology can be viewed from TP-AFM images (Figure 1F,H). Without zein confinement, the majority of PEO chains are associated with each other in a more extended manner and form extended-chain IF(n = 0) crystals. However, the d-spacing of 100% F127 pellet is 209 Å, still lower than the chain length of PEO (M_w = 4250 Da) (269 Å). This phenomenon is probably relevant to the kinetic pathway, which refers to crystallization temperature and crystallization period. Because lower or higher crystallization temperature can lead to shorter or longer fold length of crystals, the current processing temperature itself limits the growth of IF(n = 0) crystals during solvent casting.

In summary, adding F127 into zein film can efficiently overcome the brittleness and broaden the application of zein products. Different F127 loadings have a large impact upon the physical properties of the composite films, which arise from a competition between crystallization and plasticization of F127. At low F127 loading (35%), the plasticizing effect due to the interaction between PPO segments and zein domain is dominant over crystallization. The flexibility of zein film has been improved by >8-fold, whereas the surface flatness and hydrophobicity can be maintained. The limited amount of crystals is majorly composed of once-folded chain (IF = 1) PEO crystals. At high F127 loading (50% and above), the F127 crystallization results in a large quantity of lamellar structure, which surpasses the plasticizing effect. Compared to the highly ordered flat-on lamellar structure in pure F127 film, the crystallization of F127 under the confinement of zein leads to less ordered branch-like lamellar structure. A large number of the crystals are a mixture of once-folded chain (IF = 1) and extended-chain (IF = 0) PEO crystals, and the portion of extended-chain (IF = 0) PEO crystals increases with F127 loading. On the basis of the established structure−property relationship, we suggest that the optimized condition for zein/F127 composite film is 35% F127 loading, which has significantly improved the mechanical properties of zein films and broadened the applications of zein as a novel biomaterial.

■ ASSOCIATED CONTENT

Supporting Information

Additional figures. This material is available free of charge via the Internet at http://pubs.acs.org.

■ AUTHOR INFORMATION

Corresponding Author

*Phone: 1 (848) 932-5514. Fax: 1 (732) 932-6776. E-mail: qhuang@aesop.rutgers.edu.

Funding

This project was supported by the U.S. Department of Agriculture National Research Initiative (2009-35603-05075).

Notes

The authors declare no competing financial interest.

■ ACKNOWLEDGMENTS

We thank Dr. Holger Schönherr and Dr. Sanjeeva Murthy for their insightful discussion of the manuscript.

■ REFERENCES

(1) Harding, K. G.; Dennis, J. S.; von Blottnitz, H.; Harrison, S. T. L. Environmental analysis of plastic production processes: comparing petroleum-based polypropylene and polyethylene with biologically-based poly-β-hydroxybutyric acid using life cycle analysis. *J. Biotechnol.* **2007**, *130*, 57−66.

(2) Yu, L.; Dean, K.; Li, L. Polymer blends and composites from renewable resources. *Prog. Polym. Sci.* **2006**, *31*, 576−602.

(3) Andersson, C.; Jarnstrom, L.; Fogden, A.; Mira, I.; Voit, W.; Zywicki, S.; Bartkowiak, A. Preparation and incorporation of microcapsules in functional coatings for self-healing of packaging board. *Packag. Technol. Sci.* **2009**, *22*, 275−291.

(4) Lankey, R. L.; Anastas, P. T. Life-cycle approaches for assessing green chemistry technologies. *Ind. Eng. Chem. Res.* **2002**, *41*, 4498−4502.

(5) Liu, J.; Tolvgard, A.; Malmodin, J.; Lai, Z. H. A reliable and environmentally friendly packaging technology − flip-chip joining using anisotropically conductive adhesive. *IEEE Trans. Compon. Packag. Technol.* **1999**, *22*, 186−190.

(6) Shukla, R.; Cheryan, M. Zein: the industrial protein from corn. *Ind. Crop Prod.* **2001**, *13*, 171−192.

(7) Li, Y.; Xia, Q.; Shi, K.; Huang, Q. Scaling behaviors of α-zein in acetic acid solutions. *J. Phys. Chem. B* **2011**, *115*, 9695−9702.

(8) Matsushima, N.; Danno, G.; Takezawa, H.; Izumi, Y. Three-dimensional structure of maize α-zein proteins studied by small-angle X-ray scattering. *Biochim. Biophys. Acta−Protein Struct. Mol. Enzym.* **1997**, *1339*, 14−22.

(9) Tatham, A. S.; Field, J. M.; Morris, V. J.; Ianson, K. J.; Cardle, L.; Dufton, M. J.; Shewry, P. R. Solution conformational analysis of the α-zein proteins of maize. *J. Biol. Chem.* **1993**, *268*, 26253−26259.

(10) Momany, F. A.; Sessa, D. J.; Lawton, J. W.; Selling, G. W.; Hamaker, S. A. H.; Willett, J. L. Structural characterization of α-zein. *J. Agric. Food Chem.* **2006**, *54*, 543−547.

(11) Shi, K.; Kokini, J. L.; Huang, Q. Engineering zein films with controlled surface morphology and hydrophilicity. *J. Agric. Food Chem.* **2009**, *57*, 2186−2192.

(12) Shi, K.; Huang, Y. P.; Yu, H. L.; Lee, T. C.; Huang, Q. R. Reducing the brittleness of zein films through chemical modification. *J. Agric. Food Chem.* **2011**, *59*, 56−61.

(13) Lawton, J. W. Zein: a history of processing and use. *Cereal Chem.* **2002**, *79*, 1−18.

(14) Lawton, J. W. Plasticizers for zein: their effect on tensile properties and water absorption of zein films. *Cereal Chem.* **2004**, *81*, 1−5.

(15) Paul, D. R.; Barlow, J. W.; Keskkula, H. *Encyclopedia of Polymer Science and Engineering*; Mark, H. F., Ed.; Wiley: New York, 1985; Vol. *12*.

(16) Ghanbarzadeh, B.; Musavi, M.; Oromiehie, A. R.; Rezayi, K.; Rad, E. R.; Milani, J. Effect of plasticizing sugars on water vapor permeability, surface energy and microstructure properties of zein films. *LWT−Food Sci. Technol.* **2007**, *40*, 1191−1197.

(17) Santosa, F. X. B.; Padua, G. W. Tensile properties and water absorption of zein sheets plasticized with oleic and linoleic acids. *J. Agric. Food Chem.* **1999**, *47*, 2070−2074.
(18) Woods, K.; Selling, G.; Cooke, P. Compatible blends of zein and polyvinylpyrrolidone. *J. Polym. Environ.* **2009**, *17*, 115−122.
(19) Selling, G.; Biswas, A. Blends of zein and nylon-6. *J. Polym. Environ.* **2012**, *20*, 631−637.
(20) Senna, M. M.; Salmieri, S.; El-Naggar, A. W.; Safrany, A.; Lacroix, M. Improving the compatibility of zein/poly(vinyl alcohol) blends by γ irradiation and graft copolymerization of acrylic acid. *J. Agric. Food Chem.* **2010**, *58*, 4470−4476.
(21) Selling, G. W.; Sessa, D. J.; Palmquist, D. E. Effect of water and tri(ethylene) glycol on the rheological properties of zein. *Polymer* **2004**, *45*, 4249−4255.
(22) Bohorquez, M.; Koch, C.; Trygstad, T.; Pandit, N. A study of the temperature-dependent micellization of pluronic F127. *J. Colloid Interface Sci.* **1999**, *216*, 34−40.
(23) Desai, P. R.; Jain, N. J.; Sharma, R. K.; Bahadur, P. Effect of additives on the micellization of PEO/PPO/PEO block copolymer F127 in aqueous solution. *Colloid Surf. A−Physicochem. Eng. Aspects* **2001**, *178*, 57−69.
(24) Ivanova, R.; Lindman, B.; Alexandridis, P. Evolution in structural polymorphism of pluronic F127 poly(ethylene oxide)-poly(propylene oxide) block copolymer in ternary systems with water and pharmaceutically acceptable organic solvents: from "glycols" to "oils". *Langmuir* **2000**, *16*, 9058−9069.
(25) Li, Y. Q.; Shi, T. F.; Sun, Z. Y.; An, L. J.; Huang, Q. R. Investigation of sol-gel transition in Pluronic F127/D_2O solutions using a combination of small-angle neutron scattering and Monte Carlo simulation. *J. Phys. Chem. B* **2006**, *110*, 26424−26429.
(26) Desai, S. D.; Blanchard, J. In vitro evaluation of pluronic F127-based controlled-release ocular delivery systems for pilocarpine. *J. Pharm. Sci.* **1998**, *87*, 226−230.
(27) Mao, C.; Liang, C. X.; Mao, Y. Q.; Li, L.; Hou, X. M.; Shen, J. Modification of polyethylene with Pluronics F127 for improvement of blood compatibility. *Colloid Surf. B−Biointerfaces* **2009**, *74*, 362−365.
(28) Xie, Y.; Hu, N. F.; Liu, H. Y. Bioelectrocatalytic reactivity of myoglobin in layer-by-layer films assembled with triblock copolymer Pluronic F127. *J. Electroanal. Chem.* **2009**, *630*, 63−68.
(29) Wei, Z.; Hao, J. G.; Yuan, S.; Li, Y. J.; Juan, W.; Sha, X. Y.; Fang, X. L. Paclitaxel-loaded Pluronic P123/F127 mixed polymeric micelles: formulation, optimization and in vitro characterization. *Int. J. Pharm.* **2009**, *376*, 176−185.
(30) Naik, S. P.; Yamakita, S.; Ogura, M.; Okubo, T. Studies on mesoporous silica films synthesized using F127, a triblock co-polymer. *Microporous Mesoporous Mater.* **2004**, *75*, 51−59.
(31) Naik, S. P.; Yamakita, S.; Sasaki, Y.; Ogura, M.; Okubo, T. Synthesis of mesoporous silica thin film with three-dimensional accessible pore structure. *Chem. Lett.* **2004**, *33*, 1078−1079.
(32) Fairclough, J. P. A.; Yu, G.-E.; Mai, S.-M.; Crothers, M.; Mortensen, K.; Ryan, A. J.; Booth, C. First observation of an ordered microphase in melts of poly(oxyethylene)-poly(oxypropylene) block copolymers. *Phys. Chem. Chem. Phys.* **2000**, *2*, 1503−1507.
(33) Alexandridis, P. Structural polymorphism of poly(ethylene oxide)−poly(propylene oxide) block copolymers in nonaqueous polar solvents. *Macromolecules* **1998**, *31*, 6935−6942.
(34) Alexandridis, P.; Zhou, D.; Khan, A. Lyotropic liquid crystallinity in amphiphilic block copolymers: temperature effects on phase behavior and structure for poly(ethylene oxide)-*b*-poly-(propylene oxide)-*b*-poly(ethylene oxide) copolymers of different composition. *Langmuir* **1996**, *12*, 2690−2700.
(35) Matsen, M. W.; Thompson, R. B. Equilibrium behavior of symmetric ABA triblock copolymer melts. *J. Chem. Phys.* **1999**, *111*, 7139−7146.
(36) Mayes, A. M.; Delacruz, M. O. Microphase separation in multiblock copolymer melts. *J. Chem. Phys.* **1989**, *91*, 7228−7235.
(37) Mayes, A. M.; Delacruz, M. O. Concentration fluctuation effects on disorder-order transitions in block copolymer melts. *J. Chem. Phys.* **1991**, *95*, 4670−4677.
(38) Fischer, H.; Polikarpov, I.; Craievich, A. F. Average protein density is a molecular-weight-dependent function. *Protein Sci.* **2004**, *13*, 2825−2828.
(39) Johnson, W. C.; Wang, J.; Chen, Z. Surface structures and properties of polystyrene/poly(methyl methacrylate) blends and copolymers. *J. Phys. Chem. B* **2005**, *109*, 6280−6286.
(40) Ghanbarzadeh, B.; Oromiehie, A. R.; Musavi, M.; D-Jomeh, Z. E.; Rad, E. R.; Milani, W. Effect of plasticizing sugars on rheological and thermal properties of zein resins and mechanical properties of zein films. *Food Res. Int.* **2006**, *39*, 882−890.
(41) Su, Y. L.; Wang, J.; Liu, H. Z. FTIR spectroscopic investigation of effects of temperature and concentration on PEO-PPO-PEO block copolymer properties in aqueous solutions. *Macromolecules* **2002**, *35*, 6426−6431.
(42) Liu, G.; Li, J.; Shi, K.; Wang, S.; Chen, J. W.; Liu, Y.; Huang, Q. R. Composition, secondary structure, and self-assembly of oat protein isolate. *J. Agric. Food Chem.* **2009**, *57*, 4552−4558.
(43) Zhu, L.; Calhoun, B. H.; Ge, Q.; Quirk, R. P.; Cheng, S. Z. D.; Thomas, E. L.; Hsiao, B. S.; Yeh, F.; Liu, L.; Lotz, B. Initial-stage growth controlled crystal orientations in nanoconfined lamellae of a self-assembled crystalline−amorphous diblock copolymer. *Macromolecules* **2001**, *34*, 1244−1251.
(44) Chen, E. Q.; Jing, A. J.; Weng, X.; Huang, P.; Lee, S. W.; Cheng, S. Z. D.; Hsiao, B. S.; Yeh, F. J. In situ observation of low molecular weight poly(ethylene oxide) crystal melting, recrystallization. *Polymer* **2003**, *44*, 6051−6058.
(45) Cheng, S. Z. D.; Chen, J.; Barley, J. S.; Zhang, A.; Habenschuss, A.; Zschack, P. R. Isothermal thickening and thinning processes in low molecular-weight poly(ethylene oxide) fractions crystallized from the melt. 3. Molecular weight dependence. *Macromolecules* **1992**, *25*, 1453−1460.
(46) Cheng, S. Z. D.; Wu, S. S.; Chen, J.; Zhuo, Q.; Quirk, R. P.; von Meerwall, E. D.; Hsiao, B. S.; Habenschuss, A.; Zschack, P. R. Isothermal thickening and thinning processes in low-molecular-weight poly(ethylene oxide) fractions crystallized from the melt. 4. End-group dependence. *Macromolecules* **1993**, *26*, 5105−5117.
(47) Cheng, S. Z. D.; Zhang, A.; Barley, J. S.; Chen, J.; Habenschuss, A.; Zschack, P. R. Isothermal thickening and thinning processes in low-molecular-weight poly(ethylene oxide) fractions. 1. From nonintegral-folding to integral-folding chain crystal transitions. *Macromolecules* **1991**, *24*, 3937−3944.
(48) Zhang, F.; Stühn, B. Crystallization and melting behavior of low molar weight PEO−PPO−PEO triblock copolymers. *Colloid Polym. Sci.* **2007**, *285*, 371−379.